Article:
Gourgouliatos, KN (2006) On the angular momentum evolution of merged white dwarfs. Monthly Notices of the Royal Astronomical Society, 371 (3). 1381 - 1389. ISSN: 0035-8711

https://doi.org/10.1111/j.1365-2966.2006.10780.x

Mon. Not. R. Astron. Soc. **371,** 1381–1389 (2006) doi:10.1111/j.1365-2966.2006.10780.x

On the angular momentum evolution of merged white dwarfs

K. N. Gourgouliatos★† and C. S. Jeffery†
Armagh Observatory, College Hill, Armagh BT61 9DG

Accepted 2006 June 28. Received 2006 June 28; in original form 2006 April 11

ABSTRACT

We study the angular momentum evolution of binaries containing two white dwarfs (WDs) which merge and become cool helium-rich supergiants. Our object is to compare predicted rotation velocities with observations of highly evolved stars believed to have formed from such a merger, which include the R CrB and extreme He stars.

The principal case study involves a short-period binary containing a 0.6-$M_\odot$ carbon–oxygen (CO) WD, and a 0.3-$M_\odot$ He WD. The initial condition for the angular momentum distribution is defined by the orbital configuration where the secondary fills its Roche lobe.

Since mass transfer from the secondary is unstable, the WD breaks up on a dynamical time-scale. After accreting some mass, the primary is assumed to ignite helium and evolve to become a yellow supergiant with a He-rich surface. We assume conservation of angular momentum to compute the initial angular momentum distribution in a collisionless disc and subsequently in the giant envelope. At the end of shell-helium burning, the giant contracts to form a WD. We derive the surface rotation velocity during this contraction.

The calculation is repeated for a range of initial mass ratios, and also for the case of mergers between two helium (He) WDs; the latter will contract to the helium main sequence rather than the WD sequence.

Assuming complete conservation of angular momentum, we predict acceptable angular rotation rates for cool giants and during the initial subsequent contraction. However, such stars will only survive spin-up to reach the WD sequence (CO+He merger) if the initial mass ratio is close to unity. He+He merger products *must* lose angular momentum in order to reach the helium main sequence.

Minimum observed rotation velocities in extreme helium stars are lower than our predictions by at least one-half, indicating that CO+He mergers must lose at least one-half of their angular momentum, possibly through a wind during shell-helium burning, but more likely from the disc, following secondary disruption.

Key words: stars: chemically peculiar – stars: evolution – stars: rotation.

1 INTRODUCTION

Following Webbink (1984), Saio & Jeffery (2002) have demonstrated that the most probable origin for extreme helium stars is a stellar merger in a binary system containing a carbon–oxygen (CO) and a helium white dwarf (WD), although some may originate in systems containing two helium WDs (Saio & Jeffery 2000). In the first case, the product ignites helium in a shell at the surface of the CO core and expands to become a helium-rich supergiant. After the helium-burning shell burns outwards through most of the helium-rich surface layers, the star contracts to become a WD. In the second case, the helium-ignition again occurs in a shell at the core–envelope boundary, but then burns inwards, lifting the electron-degeneracy in the helium core. When the helium-burning flame reaches the centre, the star essentially becomes a low-mass helium main-sequence star.

A criticism occasionally heard (but, to our knowledge, not yet written) is that the products of such mergers should have a very high angular momentum and thus should be observed as rapid rotators. While general arguments suggest that this should not be a problem, it seemed appropriate to investigate the question more rigorously.

Previously, Saio & Jeffery (2000, 2002) examined the evolution of the internal structure of stars, following two types of WD merger. In this paper, we focus on the evolution of the angular momentum distribution from binary progenitor to final WD. We aim to set limits on the predicted rotation velocities of the merger products.

★Present address: Institute of Astronomy, The Observatories, Madingley Road, Cambridge CB3 0HA.
†E-mail: kng22@cam.ac.uk (KNG); csj@arm.ac.uk (CSJ)

2 ANGULAR MOMENTUM: GENERAL CONSIDERATIONS

The final mass of systems that become extreme helium stars does not appear to exceed 0.9 $M_\odot$ (Saio & Jeffery 2002). Assuming tidal locking for the progenitor binary, we conclude that the orbital angular momentum is dominant. We already know that angular momentum will be removed by gravitational radiation on a time-scale that depends on the initial separation of the binary and will lead to a decrease in the orbital separation (Chau 1978). For binary WDs that have a period of a few hours and an initial separation of $\sim 10^{11}$ cm $\sim 2\,R_\odot$, the time needed to merge is less than the Hubble time. Thus, we expect a significant fraction of existing close WD binaries to merge. Because of orbital decay, at some point the secondary fills its Roche lobe. The orbital period at this point can be determined from the separation and is approximately 3 min. Subsequently, mass starts to transfer from the secondary to the primary. All the transferred mass cannot be accreted on to the primary because of the Eddington limit. The mass transfer is unstable because of the inverse mass–radius relation for WDs. Hence, the secondary will break up and form a thick disc round the primary on a dynamical time-scale. For such systems, this is very short and of the order of the orbital period.

To begin with, we assume conservation of total mass. This has been demonstrated for the early evolution of WD mergers (Segretain, Chabrier & Mochkovitch 1997; Geurrero, García-Berro & Isern 2004), but not for the later stages of their evolution. In order to determine the characteristics of the angular momentum profile of the disc, we use two quantities, specific angular momentum and angular momentum density, defined in Section 3. The conservation of total angular momentum is a plausible assumption. In addition, we assume conservation of angular momentum for every single particle (or fluid element). Thus, the discussion reduces to an idealized collisionless model.

This is a conservative assumption, which effectively reduces to a worst-case scenario. In the collisionless model, the transfer of angular momentum is slow compared to the dynamical time-scale and, hence, it does not have important effects. The opposite assumes a model in which collisions are important, producing a viscous disc. The problem of angular momentum transport in a viscous disc has been approached already (Lynden-Bell & Pringle 1974), where it was shown that 'the angular momentum is steadily concentrated onto a small fraction of the mass which orbits at greater and greater radii while the rest is accreted onto the central body' on an approximately dynamical time-scale. The problem for the viscous disc approximation is that the accretion rate for the surviving WD then becomes very high and it is not clear whether subsequent evolution will lead to the assimilation of this mass or its complete ejection by radiation pressure. Consequently, we have started with the collisionless model to see whether it, too, faces major obstacles.

Using the above assumption, we propose an angular momentum distribution profile for the disc. In the purely collisionless model, as will be shown, the inner radius of the disc is approximately twice the radius of the primary. The intervening gap will prevent accretion. In real systems, random collisions will broaden the angular momentum profile. We will simulate this by applying a Gaussian smoothing function, where the width of the Gaussian may be considered a representative of the frequency of the collisions. Note that this procedure does not change the total angular momentum of the system.

Since the disc was created from the decomposition of the secondary, which was a helium WD, helium will be its dominant constituent. Following Saio & Jeffery (2002), after a small quantity ($0.004\,M_\odot$) of helium is accreted by the primary, helium-ignition occurs at the base of the accreted layer. This energy source forces the star to expand to become a giant. Models indicate that the radius of the giant will be two orders of magnitude greater than that of the disc, initially about $60\,R_\odot$.

A simple model for the angular momentum distribution in the giant can be obtained by assuming that each cylindrical element in the disc forms a spherical shell conserving its angular momentum. In order to describe the density profile of the giant, we assume it to consist of a degenerate core, that is the CO WD, and a convective envelope. In the fully conservative case, the final mass of the convective envelope is equal to the mass of the initial disc, and hence of the helium secondary. Therefore, we can describe an angular velocity distribution for the star.

Following calculation of the angular velocity distribution in the giant merger product, we investigate how contraction affects the rotation. After helium-burning is completed, the stars will contract, and hence rotate more quickly. The question is whether or not their rotation will approach the critical breakup velocity and what the consequences might be.

For the CO+He WD merger, we investigate three possible cases. In the first case, the central region rotates as a rigid body and the angular velocity profile of the envelope depends on the initial conditions, meaning the disc angular momentum distribution. In the second case, 25 per cent of the convection zone near the surface, as well as the central region, rotates as a rigid body, whereas there is differential rotation in the intermediate region. In the third case, we examine the case of completely rigid body rotation. This should be the ultimate equilibrium state, since no shear torques occur that could lead to angular momentum transfer (Lynden-Bell & Pringle 1974; Pringle 1981); however, it is not likely to be achieved, since it is a slow process.

Using the above assumptions we will model the angular momentum evolution of a binary which consists initially of two WDs. For the structure of the WDs, we will adopt the models described by Chandrasekhar (1958). For the principal calculation, we will consider the primary to be a CO WD with mass $0.6\,M_\odot$ and radius $0.013\,R_\odot$ and the secondary a helium (He) WD with mass $0.3\,M_\odot$ and radius $0.021\,R_\odot$ (Vennes, Fontaine & Brassard 1995; Panei, Althaus & Benvenuto 2000). In addition, we will consider CO+He binaries with masses of $0.7\,M_\odot + 0.2\,M_\odot$ and $0.5\,M_\odot + 0.4\,M_\odot$, in order to see the dependence, if any, of the angular velocity on the initial mass ratio. We also compute appropriate quantities for a number of He+He WD configurations. Finally, the results of these calculations are compared with observed angular velocities in extreme helium stars.

3 ORBITAL DECAY TO ROCHE LOBE

According to the General Theory of Relativity, two orbiting masses M_1 and M_2 with a separation α will radiate angular momentum at a rate (Landau & Lifshitz 1958):

$$\frac{\dot{J}}{J} = -\frac{32}{5}\frac{G^3}{c^3}\frac{M_1 M_2 M}{\alpha^4}, \tag{1}$$

where G is the gravitational constant, c the speed of light, and $M = M_1 + M_2$ is the total mass of the system. Due to angular momentum loss, their orbits will decay. The total angular momentum of a tidally locked system will be

$$J_{\rm tot} = J_1^{\rm o} + J_1^{\rm s} + J_2^{\rm o} + J_2^{\rm s}, \tag{2}$$

where the superscripts 'o' and 's' refer to orbital and spin angular momentum, respectively, and the subscripts 1 and 2 refer to the primary and the secondary, respectively. We can express the orbital angular momentum in the frame of reference of the centre of mass:

$$J_{\rm tot}^{\rm o} = M_1 M_2 \sqrt{\frac{G\alpha}{M}}, \tag{3}$$

where M is the total mass of the system. Spin angular momentum can be expressed as

$$J_{\rm tot}^{\rm s} = (I_1 + I_2)\omega, \tag{4}$$

where ω is the angular velocity and I refers to the moment of inertia. Moments of inertia can be evaluated from the density profile of the stars. However, some distortions may occur that alter it slightly (James 1964; Tassoul 1978). The angular velocity is given by

$$\omega = \sqrt{\frac{GM}{\alpha^3}}. \tag{5}$$

Substituting angular momentum expressions from equations (3) and (4) and differentiating with respect to α, we obtain the following expression:

$$\frac{\dot{J}}{J} = \left(\frac{M_1 M_2}{2(M\alpha)^{1/2}} - \frac{3 I_{\rm tot} M^{1/2}}{2\alpha^{5/2}}\right) \times \left(\frac{M_1 M_2 \alpha^{1/2}}{M^{1/2}} - \frac{I_{\rm tot} M^{1/2}}{\alpha^{3/2}}\right)^{-1} \dot{\alpha}. \tag{6}$$

As the orbit decays, the equipotential surface surrounding the two stars (Roche lobes) shrinks until one component exactly fills its own lobe. The Roche lobe radius is given by (Eggleton 1983):

$$\alpha_{\rm L} = \frac{0.49 q^{2/3}}{0.6 q^{2/3} + \ln(1 + q^{1/3})}, 0 < q < \infty \tag{7}$$

where q is the ratio of the mass of the primary to the mass of the secondary.

For the $0.6 + 0.3\,{\rm M}_\odot$ system defined above, the secondary will fill its Roche lobe when the orbital separation is $0.067\,{\rm R}_\odot$. From equations (1) and (6), we can estimate the orbital decay time-scale. Assuming an initial separation of $1.5\,{\rm R}_\odot$, which corresponds to an orbital period of 5 h, we obtain a time-scale of 4×10^9 yr, which is less than a Hubble time. We note that observations of an increasing number of such close binary WDs (Paczynski 1990; Marsh 1995; Napiwotzki et al. 2005) are commensurate with estimated merger rates (Iben, Tutukov & Yungelson 1996; Nelemans et al. 2001).

4 DISC FORMATION

When the secondary fills its Roche lobe, it disintegrates and its remnants form a disc. We will use the assumption of angular momentum conservation to determine the mass distribution in the disc. First, we construct two useful quantities for the distribution of angular momentum in the secondary. The first is the angular momentum per unit mass, hereafter specific angular momentum, which will be expressed as $\mathrm{d}J(m)/\mathrm{d}m$, assuming the system shows cylindrical symmetry. Since we generally assume a collisionless model, this quantity remains constant throughout the problem, unless some mass is lost. The other quantity is the angular momentum contained within a distance r from the centre of the system, hereafter angular momentum density, and will be expressed as $\mathrm{d}J(r)/\mathrm{d}r$. It depends strongly on the geometry of the problem. When the secondary fills its Roche lobe, it expresses the angular momentum contained in a thin slice of the star at a distance r from the rotation axis of the primary. The slice lies perpendicular to the radial vector that points from the centre of the primary to the centre of the secondary. In the case of the disc, $\mathrm{d}J/\mathrm{d}r$ expresses the angular momentum carried by a thin cylindrical shell of radius r. In the case of the giant star, it expresses the angular momentum carried by a spherical shell at a distance r from the rotation axis of the star.

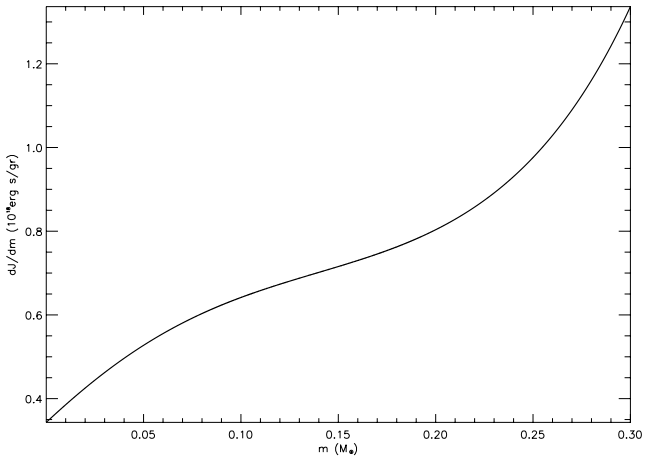

Figure 1. The specific angular momentum $\mathrm{d}J/\mathrm{d}m$. It remains constant throughout the problem, since we examine a collisionless model.

From the definition of angular momentum, a particle of mass $\mathrm{d}m$ that lies at a distance r from the primary and moves at an angular velocity ω has angular momentum

$$\mathrm{d}J = r^2 \omega\, \mathrm{d}m. \tag{8}$$

Integrating the specific angular momentum over mass and the angular momentum density over distance, we obtain the total angular momentum of the system. For our example conditions, it is 4.5×10^{50} erg s and remains constant throughout the evolution of the system, unless some mass is lost. We can easily obtain from the orbital elements the angular velocity of the secondary, when $\alpha = \alpha_{\rm L}$, to be $\omega = 0.0346\,{\rm rad\,s^{-1}}$. The density of the secondary can be approximated by a polynomial function that fits the data given by Chandrasekhar (1958) for the structure of WDs. Hence, we can derive the specific angular momentum (Fig. 1) and the angular momentum density (Fig. 2) for the system immediately before disruption of the secondary.

After disruption of the secondary, a disc is formed. Since the disc is supported by gravity, we assume it to be Keplerian. Therefore, the angular velocity distribution can easily be determined to first order, ignoring the self-gravitating effects of the disc itself:

$$\omega(r) = \sqrt{\frac{GM_1}{r^3}}. \tag{9}$$

The angular momentum for a particle of mass m, performing circular motion of radius r, is $J = m\omega r^2$. Particles that carry less of the angular momentum at the binary stage lie at the front surface of the star (i.e. face-on to the primary). The angular momentum of these particles will determine the inner radius of the disc. In our case, this is $r_{\rm in} = 0.022\,{\rm R}_\odot$. We can use the same argument for the outer radius of the disc. In that case, we evaluate the angular momentum of a particle at the rear surface of the secondary. We conclude that it is $r_{\rm out} = 0.305\,{\rm R}_\odot$. If we take into account the self-gravitating effect of the mass stored in the disc, the outer radius is decreased by 30 per cent to $r_{\rm out} = 0.203\,{\rm R}_\odot$, whereas the inner radius will remain unaffected. This may be shown by a first-order approximation. Assuming that

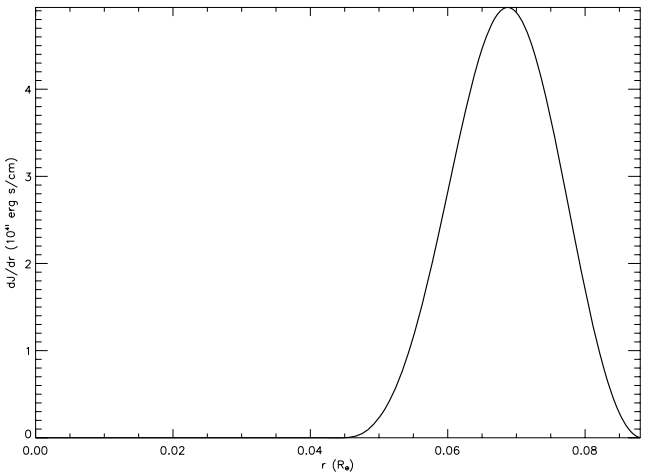

Figure 2. The angular momentum density $\mathrm{d}J/\mathrm{d}r$ at the Roche lobe stage. We can see that most angular momentum is carried at a distance slightly farther from the centre of the secondary ($0.067\,\mathrm{R}_\odot$). This is because $\mathrm{d}J/\mathrm{d}r$ is proportional to the mass contained inside a slice of the star and to the square of the distance. This product has a maximum at $0.069\,\mathrm{R}_\odot$ from the centre of the primary.

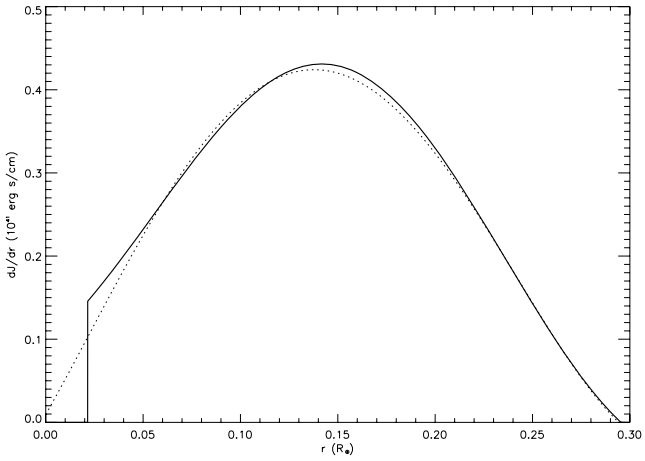

Figure 3. The angular momentum density $\mathrm{d}J/\mathrm{d}r$ of the disc. Angular momentum is spread in a more extended region than it was at the Roche lobe stage. If we take into account the self-gravitation of the disc, then its size decreases, but the total angular momentum cannot change. Since we have a collisionless model, no mass is scattered closer to the star than $r_{\mathrm{in}} = 0.22\,\mathrm{R}_\odot$. The spin angular momentum of the primary has been neglected, since it is three orders of magnitude smaller than the angular momentum of the disc. The dotted line corresponds to the convolution of $\mathrm{d}J/\mathrm{d}r$ with a Gaussian with $\sigma = 0.005\,\mathrm{R}_\odot/\sqrt{2}$.

a particle of unit mass carrying angular momentum J lies in the gravitational field of a mass M, then at radius r, the attractive force is GM/r^2. Including the gravitational field of a disc of mass m, the central force on the test particle, now at radius r', is $G(M + m)/r'^2$. Since J is constant, the ratio of radii (for $m = 0.3\,\mathrm{M}_\odot$, $M = 0.6\,\mathrm{M}_\odot$) is $r'/r = 2/3$. In higher order, the geometry of the disc must be considered, but this does not affect the angular momentum calculation.

Whether we use the first or the second approximation for the angular momentum density will have no effect on our final results for the rotation of the giant star, since the specific angular momentum does not change. The choice only affects the angular momentum density at the disc stage (Fig. 3).

During the formation of the disc, collisions may take place. These will broaden the angular momentum distribution, in particular to scatter material into the region $r < r_{\mathrm{in}}$. Angular momentum will also be transferred to outer parts of the disc which will become more extended. In order to simulate the effect of these collisions, we convolve the angular momentum functions ($\mathrm{d}J/\mathrm{d}r$) with a Gaussian of width $\sigma = 0.005\,\mathrm{R}_\odot/\sqrt{2}$, where the width of the Gaussian may be taken to represent the overall efficiency of the collisions. The resulting density distribution demonstrates that only a very modest collisional redistribution of angular momentum is required to bring disc and star into contact (Fig. 3).

5 GIANT STAGE

Following disc formation and providing that gas has been scattered to $r < r_{\mathrm{in}}$, helium will be accreted from the disc on to the surface of the former primary, which becomes the degenerate core of the merged star. Saio & Jeffery (2002) adopted an accretion rate of roughly half the Eddington rate. After $\sim 0.029\,\mathrm{M}_\odot$ is accreted, a helium flash occurs. This leads the star to expand and form a yellow giant. The expansion is rather rapid and lasts for only 200 yr. The radius of the giant initially reaches $\sim 60\,\mathrm{R}_\odot$. This stage of evolution may correspond to some hydrogen-deficient carbon giants and the coolest of the R CrB stars (Saio & Jeffery 2002). The radii of some models do exceed this value, so we surmise that the surface rotation will be lower than that deduced here. However, assuming a conservative distribution of specific angular momentum, spin-down during expansion and spin-up during contraction should lead to a similar final result.

Our objective is to predict the angular velocity profile for such a giant. In order to model its density profile, we expect it to consist of a degenerate core and a convective envelope. Using tables from Chandrasekhar (1958), fitted with a fifth-order polynomial, we approximate the envelope as a polytrope of index $n = 3/2$ and express the density as a function of r that fits the numerical results of the Lane–Emden equation for $n = 3/2$ (Mohan & Al-Bayaty 1980). We assume that initially no angular momentum is transferred between the various parts of the star. Therefore, we first make the approximation that the outside surface of the star will form the outside shell of the star, whereas the inner parts of the disc will stay near the core, and that there is no change in the specific angular momentum.

However, it is also possible that helium-shell ignition occurs before the disc has been fully accreted, so that the material which was accreted first becomes the surface of the expanding giant, whereas the disc survives for sometimes *inside* the giant envelope. Subsequent accretion, or the disintegration of the disc, feeds mass into the interior of the giant, close to the core–envelope boundary. We will examine this case as well, assuming that the outer layer of the giant, with a mass equal to the burning shell, comes from the inner part of the disc and the remainder of the envelope comes from the disintegration of the disc and obeys cylindrical symmetry.

We neglect differential rotation within a shell, so a thin spherical shell of mass $\mathrm{d}m$ at a distance r from the centre of the star rotates as a rigid body with moment of inertia

$$I = \frac{2}{3} r^2\,\mathrm{d}m. \tag{10}$$

The choice of cylindrical shells, rather than spherical, is made primarily on grounds of mathematical simplicity. There is some evidence (e.g. the Sun) that rotation may be a function of latitude – possibly suggesting cylindrical symmetry. It will be seen, however,

that the difference between the extreme cases of rigid-body and differential rotation is sufficiently small that the choice of geometry in the latter is unlikely to be important.

We examine a number of cases.

Case 1: rigid core + differential envelope

The first case involves two regions including a central region containing the degenerate core and a shell of the star's envelope of width $0.045\,R_\odot$, performing rigid body rotation. Assuming that the core rotates with the original angular velocity of the primary WD, this is the critical radius for rigid-body rotation. Beyond this, the envelope is assumed to rotate differentially according to the angular momentum distribution determined by the disc stage (Fig. 4). The outer boundary to the region of solid body rotation is chosen in order to avoid the possibility of having a rotational velocity that exceeds the orbital velocity at this point. This scenario predicts an angular velocity on the outer layer of the star of $1.15 \times 10^{-7}\,\mathrm{rad\,s^{-1}}$, corresponding to an equatorial surface velocity $v_{\rm eq} = 4.95\,\mathrm{km\,s^{-1}}$. There is a slight discontinuity between the two regions described above. It can be considered as a surface of infinite gradient $\mathrm{d}\omega/\mathrm{d}r$. In such a case, the transfer of angular momentum will be very fast and the discontinuity will vanish. This will be the initial stage in the giant's angular momentum evolution (Fig. 5). Fig. 6 shows the ratio of centrifugal force to gravitational force as a function of radius. This drops rapidly outside the core, so rotation should not significantly affect the structure of the envelope, although it may produce a slightly ellipsoidal star.

Case 2: rigid core + transition layer + rigid envelope

In the second case, we divide the star into three regions: the first is the core and a thin layer that rotates as a rigid body as before, the second region lies between $0.045\,R_\odot$ and $45\,R_\odot$, where the star rotates differentially as before, and the third region lies between $45\,R_\odot$ and the surface. This boundary was chosen arbitrarily in order to represent a case someway between the extremes discussed in cases 1 and 3. We expect that near the surface, convection may be strong enough that mixing will cause these outer layers to rotate as a rigid body (Fig. 7). Therefore, the angular velocity for the surface and the outer convection zone is $1.27 \times 10^{-7}\,\mathrm{rad\,s^{-1}}$, corresponding to $v_{\rm eq} = 5.33\,\mathrm{km\,s^{-1}}$. There is also a slight discontinuity at the 45-$R_\odot$ boundary of $\delta\,\omega = 1.2 \times 10^{-8}\,\mathrm{rad\,s^{-1}}$. This represents an intermediate case, since angular momentum is transferred within the star.

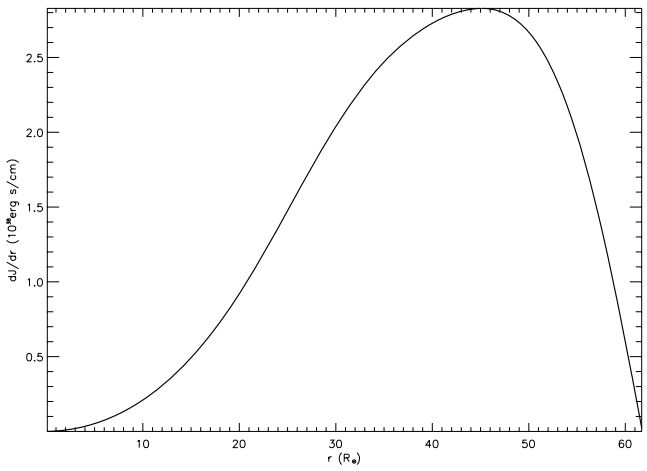

Figure 4. The angular momentum density $\mathrm{d}J/\mathrm{d}r$ of the convective envelope of the giant.

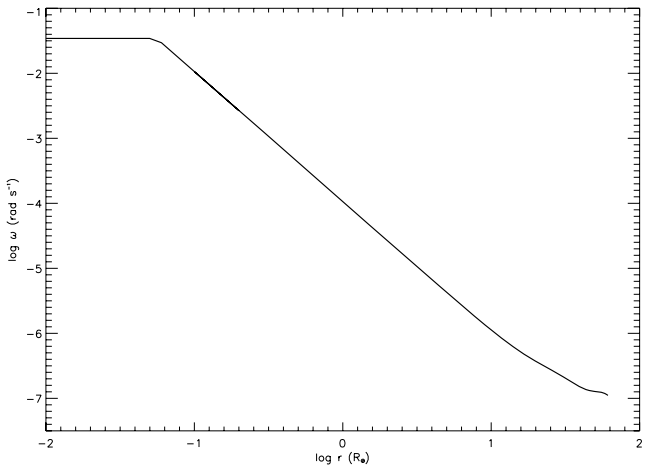

Figure 5. Logarithmic plot of the angular velocity ω at the giant stage as a function of the distance from the rotation axis. The central region rotates as a rigid body, whereas angular velocity falls with distance from the axis.

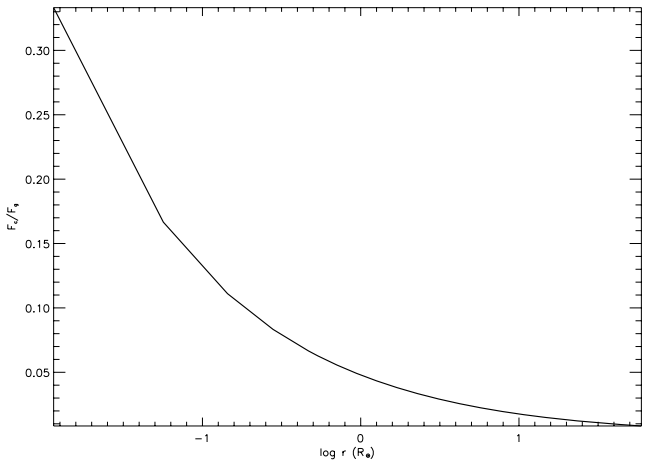

Figure 6. The ratio of centrifugal force to gravitational force as a function of radius for case 1. The plot shows only the differentially rotating stellar envelope.

Case 3: rigid body rotation

The third case to consider is that of rigid body rotation for the whole star. Shear torques may transfer angular momentum outwards from the core to the outer layers and thus make them move faster, whereas the inner layers will rotate more slowly. Rigid body rotation is the equilibrium state, since it is the lowest-energy state for an object with determined angular momentum (Lynden-Bell & Pringle 1974; Pringle 1981) and contains no shear torques that will transfer angular momentum. However, this equilibrium is not achieved by real stars even on very long time-scales, as illustrated by the Sun. It is unlikely to occur on the very short time-scales and very low-density envelopes under consideration here. Nevertheless, it represents an important limiting case in which most of the angular momentum is carried in the outer layers of the star. We can easily evaluate the moment of inertia for the giant star by integrating equation (10)

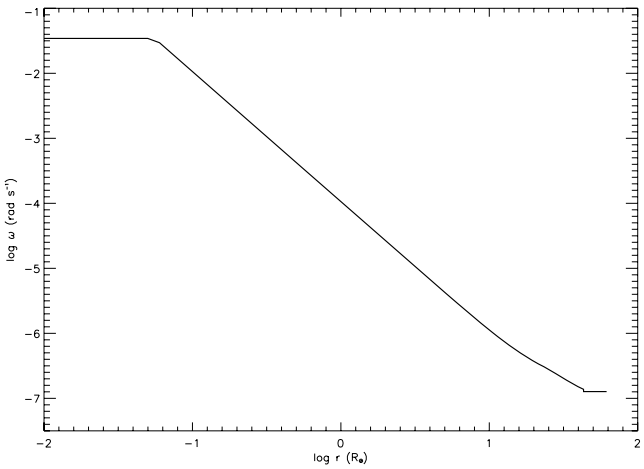

Figure 7. The angular velocity ω of the disc, in the second scenario. The central and the intermediate region rotate as in the previous case (Fig. 6); however, there is a layer at the outer part of the convective envelope that rotates as a rigid body. There are two slight dicontinuities at the boundaries of the three regions.

throughout the star to obtain $I_{\rm giant} = 2.85 \times 10^2\,{\rm g\,cm^2\,M_\odot^{-1}\,R_\odot^{-2}}$. From conservation of angular momentum, we find that $J_{\rm giant} = 4.71 \times 10^{-5}\,{\rm erg\,s\,M_\odot^{-1}\,R_\odot^{-2}}$. Therefore,

$$\omega_{\rm giant} = \frac{J_{\rm giant}}{I_{\rm giant}}, \tag{11}$$

which is $1.64 \times 10^{-7}\,{\rm rad\,s^{-1}}$ corresponding to $v_{\rm eq} = 7.1\,{\rm km\,s^{-1}}$. This case represents the fastest rotation of the surface layers and sets an upper limit for the observed rotation velocity.

We conclude that the equatorial surface velocities do not depend strongly on the details of the model. Using the above argument, we can define an upper limit on the angular momentum that corresponds to rigid body rotation. Any velocity observed should be less than this limit. We have not taken into account any losses of angular momentum due to mass ejection. Such phenomena will lead to lower angular momentum and therefore lower angular velocity. In the polytropic density profile, we have neglected any term from rotation; this gives a good approximation, since the linear velocity of circular motion due to the gravitational field of the star at a radius equal to the giant star radius is $53\,{\rm km\,s^{-1}}$, or about one order of magnitude greater than the velocities we found. In addition, any distortion caused by rotation will increase the moment of inertia of the star and decrease the angular velocity, supporting the statement that rigid body rotation of a spherical body represents the maximum possible equatorial surface velocity.

Case 4: rigid core $0.87\,{\rm M_\odot}$ + differential envelope

The fourth case can be considered as a combination of cases 1 and 3. During evolution as a giant, the helium-burning shell eats up the envelope, so the core mass increases, while the core radius remains virtually unchanged. Conversely, the envelope retains the same radius but a drastically reduced mass. We consider a final configuration in which the envelope mass is $0.03\,{\rm M_\odot}$. The moment of inertia of the core increases but cannot exceed $1.4 \times 10^{-5}\,{\rm g\,cm^2}$. Even in this case, no more than 15 per cent of the total angular momentum can be stored in the core before the core reaches its breakup limit. Therefore, the envelope will have to rotate about 30 times faster than in case 1.

Such rotation is extremely fast and seems implausible; at least, it is not observed. The problem is that, to be conservative, angular momentum must be transferred into the core at the same time as the envelope is ingested. However, once the core reaches breakup velocity, the transfer of angular momentum becomes impossible, so the momentum must stay in the envelope, creating a paradox. Interestingly, this parallels the case for the viscous disc (Lynden-Bell & Pringle 1974) in which angular momentum is expelled outwards as mass migrates inwards.

This calculation therefore strongly suggests that if stable shell-burning giants are to be produced by WD mergers, then a large fraction of the total angular momentum must be dissipated from the disc *before* it is accreted on to the primary.

While this case is the most interesting and realistic of the four considered, it has presented a paradox for the transfer of angular momentum from the envelope to the growing core. The consequences of this deserve more attention than we are currently equipped with to explore.

6 HOMOLOGOUS CONTRACTION

Having considered the angular momentum distribution of a star as it evolves from a WD binary through to being a giant, we next consider the angular velocity distribution following shell-helium extinction and the subsequent contraction at constant luminosity towards the WD cooling track.

Since the core is degenerate, we need to consider only the evolution of the envelope, which we will consider to contract homologously. A simple model can be developed by assuming that the star rotates as a rigid body (case 3).

However, no crucial differences will be found if we assume differential rotation, as demonstrated in the previous section. The only effect would be to find lower surface equatorial velocities. In order to become a WD, the star needs to reduce in size by a factor of $\sim 2 \times 10^{-4}$. Leaving the core unaffected, while the star shrinks, we evaluate the angular velocity and the equatorial surface velocity corresponding to this rotation. We plot the angular velocity (Fig. 8) and the ratio of the linear equatorial rotation velocity, $v_{\rm eq}$, to the linear velocity of a particle moving on a circular orbit, $v_{\rm orb}$, at the surface:

$$\lambda = \frac{v_{\rm eq}}{v_{\rm orb}} \tag{12}$$

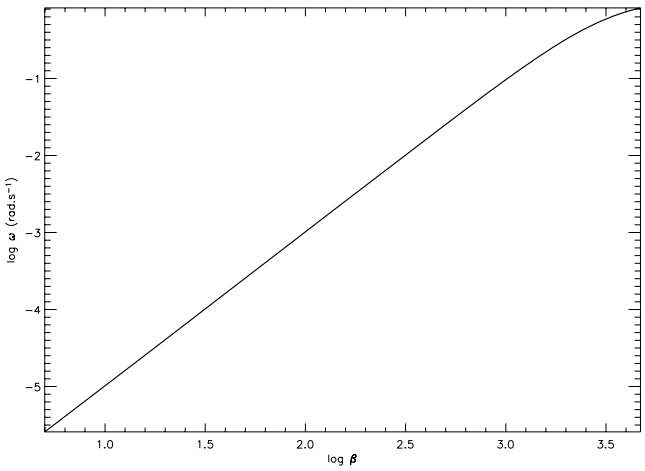

Figure 8. Logarithmic plot of the angular velocity ω as the star contracts by a fraction $\beta = R_0/R$. R_0 is the radius of the giant before contraction.

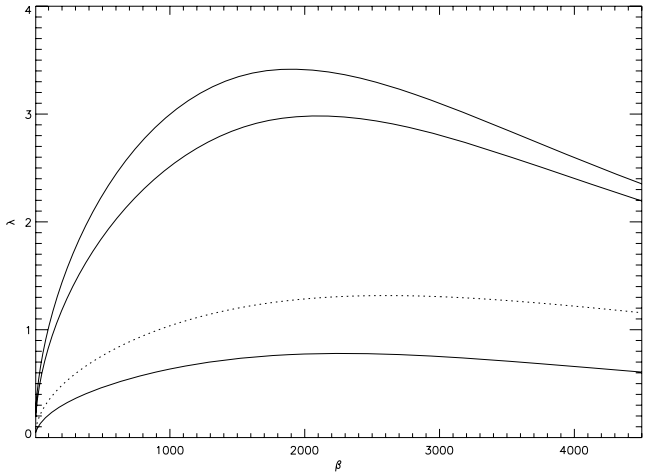

Figure 9. The ratio of the velocity due to rotation to the velocity of the circular orbit on the surface of the star, λ, as a function of β which is the contraction factor for three pairs of masses of the progenitors; from top to bottom: $0.7\,M_\odot + 0.2\,M_\odot$, $0.6\,M_\odot + 0.3\,M_\odot$ and $0.5\,M_\odot + 0.4\,M_\odot$. Contraction cannot continue if λ approaches unity. In order to become a WD, the star needs to contract by a factor of about 5×10^3. We can see that for progenitor masses of $0.5\,M_\odot + 0.4\,M_\odot$, contraction can reach the WD radius, whereas for the other two cases angular momentum needs to be removed. The dotted line corresponds to the model of a merger with progenitor masses of $0.6\,M_\odot + 0.3\,M_\odot$ where 50 per cent of the secondary mass is lost.

(Fig. 9, middle curve). The quantity on the horizontal axis is the ratio β of the radius of the giant, R_0, to the radius during contraction, R. The moment of inertia decreases with the square of the radius, which will lead the star to rotate faster (Fig. 8). Note that contraction implies increasing β.

Problems occur when the rotation velocity approaches or exceeds the value of velocity for a circular orbit ($\lambda \gtrsim 1$). Thus, when the star contracts to ∼0.007 times its initial radius, the two velocities become equal and the star cannot shrink anymore, unless some angular momentum is lost. At this point, the velocity is of the order of $\sim 10^2\,\mathrm{km\,s^{-1}}$. This is much lower than the speed of light and relativistic effects may be ignored.

7 AN ANGULAR MOMENTUM PROBLEM?

So far we have examined a fully conservative scenario from the Roche lobe stage and onwards for a $0.6\,M_\odot + 0.3\,M_\odot$ binary. However, much energy is ejected at the breakup of the secondary. Some of this energy may be deposited in the disc as thermal kinetic energy, whereas some material of high angular momentum is likely to leave the system, although the maximum possible mass lost has been shown to be small (Han & Webbink 1999).

We therefore examine whether the contraction of the giant can proceed conservatively if some mass (and hence its associated specific angular momentum) is ejected. Although this is contrary to our initial assumptions and previous numerical results (Segretain et al. 1997; Han & Webbink 1999; Geurrero et al. 2004), this mass ejection is treated as taking place during the phase of disc formation. This approximation avoids numerical complications which are beyond the scope of this paper, but allows us to obtain a rough estimate of the resulting configurations when mass loss is taken into account.

We have solved the problem for the cases where 1, 5, 10, 25 and 50 per cent of the mass of the secondary is ejected during the merger process. In all cases, the giant cannot contract to the radius of a WD. Fig. 9 includes the case in which 50 per cent of the mass of the secondary is ejected. In this test case, two-thirds of the total angular momentum is removed, since particles carrying more angular momentum are more likely to escape. λ reaches unity when $\beta \approx 1000$, which means that the star can reach a small size (10^{-3} times its original), but not less than five times the required WD radius.

In order to investigate the role of the initial conditions, we have solved the problem for various relative masses of the WD binary components. We have plotted the ratio of the equatorial rotation velocity to the surface orbital velocity (λ) for progenitor binaries of $0.7 + 0.2\,M_\odot$ and $0.5 + 0.4\,M_\odot$ in addition to the test case of $0.6 + 0.3\,M_\odot$ (Fig. 9). When $\lambda \gtrsim 1$, contraction cannot proceed. We see that for mass ratios nearer to unity the star *can* contract to WD size without the need for additional angular momentum loss. This is expected, since such systems need to lose more angular momentum before the secondary star fills its Roche lobe. This is because the WD radius varies inversely with mass, so more massive WDs will have smaller radii and will fill their Roche lobes later. Close orbits involve less angular momentum, of course, and their products will rotate more slowly.

Therefore, conservation of angular momentum does present a problem for the WD merger model in most, but not all, cases. The problem arises either during helium-shell burning, when angular momentum has to be transferred to the envelope to avoid the core reaching breakup velocity, or during contraction, when the surface reaches breakup velocity.

8 HELIUM+HELIUM WHITE DWARF MERGERS

The case of merger between two helium WDs is initially identical to that of the CO+He merger (Saio & Jeffery 2000). After shell-helium ignition, the star expands to become a giant, and the envelope is capable of storing substantial angular momentum. However, the star evolves to become a helium main-sequence star on a short timescale (Iben 1990). The case is analogous to the CO+He merger which must spin-up during contraction to become a WD.

We have calculated rotation rates for helium main-sequence stars arising from a number of initial configurations. The final configuration is an $n = 5/2$ polytrope with overall dimensions given by Paczynski (1971).

Table 1 shows the run of the moments of inertia I, total angular momenta J, and angular and linear equatorial rotation velocities (ω, $v_{\rm rot}$) for a series of initial configurations (M_1, M_2). The predicted values for $v_{\rm rot}$ are very high and, in most cases, substantially exceed the critical orbital velocity at the surface ($v_{\rm orb}$). Clearly, such stars cannot exist and it is necessary to find a mechanism for expelling angular momentum at an earlier stage. In this case, losing some angular momentum at the breakup of the secondary when it fills its Roche lobe is likely, since the total mass of the binary and the binding energy is lower. In addition to this, less massive WDs have larger radii and fill their Roche lobe earlier. This will enable mass carrying angular momentum to escape the system earlier.

9 OBSERVED ROTATION RATES

Observations suggest modest rotation velocities for extreme helium stars. Measurements of the projected rotation velocity $v_{\rm eq} \sin i$ for 10 objects have been obtained by fitting line profiles to absorption lines in the optical spectrum (Table 2). For small values of

Table 1. Theoretical predictions for the rotation of helium main-sequence stars produced by He+He WD mergers for various combinations of initial masses.

M ($M_\odot$)	$M_1 + M_2$ ($M_\odot$)	I ($10^{-3}\,M_\odot\,R^2_\odot$)	J (10^{-5} erg s $M_\odot^{-1}\,R_\odot^{-2}$)	ω (rad s^{-1})	$v_{\rm rot}$ (10^3 km s^{-1})	$v_{\rm orb}$ (10^3 km s^{-1})
0.5	0.3+0.2	1.16	2.53	0.044	3.2	0.95
0.5	0.4+0.1	1.16	1.71	0.030	2.2	0.95
0.7	0.4+0.3	3.18	3.83	0.012	1.2	0.96
0.7	0.5+0.2	3.18	3.18	0.010	1.0	0.96

Table 2. Projected rotation velocities for extreme helium stars.

Star	$T_{\rm eff}$ (K)	$\log g$	$v_{\rm eq}\sin i$ (km s^{-1})	R ($R_\odot$)	$\omega \sin i$ (10^6 rad s^{-1})	Reference
FQ Aqr	8750 ± 300	0.3 ± 0.3	20 ± 5	136 ± 96	0.22 ± 0.17	Pandey et al. (2006)
HD168476	$13\,500 \pm 500$	1.6 ± 0.25	25 ± 5	23 ± 13	1.6 ± 1.0	Pandey et al. (2006)
LSS 99	$15\,330 \pm 500$	1.9 ± 0.25	30 ± 5	16 ± 9	2.9 ± 1.7	Jeffery et al. (1998)
HD124448	$15\,500 \pm 500$	1.9 ± 0.25	4 ± 5	16 ± 9	0.38 ± 0.5	Pandey et al. (2006)
LSS 4357	$16\,130 \pm 500$	2.0 ± 0.25	45 ± 5	14 ± 8	4.9 ± 2.8	Jeffery et al. (1998)
LS II + 33° 5	16180 ± 500	2.0 ± 0.25	45 ± 5	14 ± 8	4.9 ± 2.8	Jeffery et al. (1998)
V1920 Cyg	$16\,300 \pm 900$	1.7 ± 0.25	40 ± 5	23 ± 13	2.6 ± 1.5	Pandey et al. (2006)
BD + 10° 2179	16900 ± 500	2.55 ± 0.2	18 ± 5	6 ± 3	4.7 ± 2.5	Pandey et al. (2006)
LSE 78	$18\,000 \pm 700$	2.0 ± 0.1	20 ± 5	15 ± 3	2.0 ± 0.7	Jeffery (1993)
DY Cen	$19\,500 \pm 500$	2.15 ± 0.1	20 ± 5	13 ± 3	2.4 ± 0.8	Jeffery (1993)

$v_{\rm eq}\sin i$, these may have been overestimated because of the difficulty of deconvolving instrumental and rotation broadening profiles in the observed spectra. Table 2 also gives the measured values of $T_{\rm eff}$ and $\log g$. By assuming a core mass–shell luminosity ($M_{\rm c}$–$L_{\rm s}$) relation (cf. Saio & Jeffery 1988), the latter may be combined to estimate both a mass and a radius for the extreme helium stars. Hence, we can obtain the projected (minimum) angular rotation velocity $\omega \sin i$. We can normalize the relative radii by assuming a minimum $T_{\rm eff,0}$ before contraction at constant luminosity, and hence derive $\beta = R_0/R = (T_{\rm eff}/T_{\rm eff,0})^2$. We have adopted $T_{\rm eff,0} = 5000$ K, the value at which post-merger giants commence their contraction (Saio & Jeffery 2002). A different value would impose a horizontal offset on to Fig. 10, which demonstrates an overall increase in $\omega \sin i$ with increasing β (and hence with increasing $T_{\rm eff}$). It is interesting that the maximum slope represented by these data corresponds to the spin-up of a homologously contracting star, $\omega \propto R^{-2}$, as theory predicts.

The projected rotation rates are all smaller than the maximum rate predicted by theory assuming complete conservation of angular momentum through the WD merger. Assuming a random distribution of inclination angles, the average rotation rates should be $\pi/4$ times the maximum rates. The observed rates are less than one-third of the maximum rate. This implies that at least half of the angular momentum must have been lost, either during the merger process or while the star was a cool giant, for example, in a wind.

The minimum rotation rate as a fraction of breakup velocity $\lambda_{\rm min} = v_{\rm eq}\sin i/v_{\rm orb}$ can also be checked using the same estimates for radius (Fig. 11). All objects are currently slow rotators ($v_{\rm eq}\sin i$ for FQ Aqr is probably overestimated for the reasons given above).

In other words, the observed rotation rates for extreme helium stars are consistent with homologous contraction of the envelope at constant luminosity. They are not consistent with complete conservation of angular momentum during the WD merger. With angular velocities less than one-third the predicted rates, the likelihood of

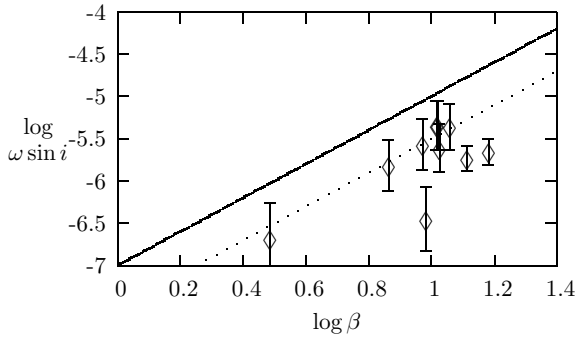

Figure 10. Projected angular rotation $\log \omega \sin i$ as a function of relative inverse radius β for extreme helium stars. The dotted line represents a homologous contraction, that is, $\omega \propto 1/R^2$, and the solid line represents the maximum theoretical rotation rate shown in Fig. 8.

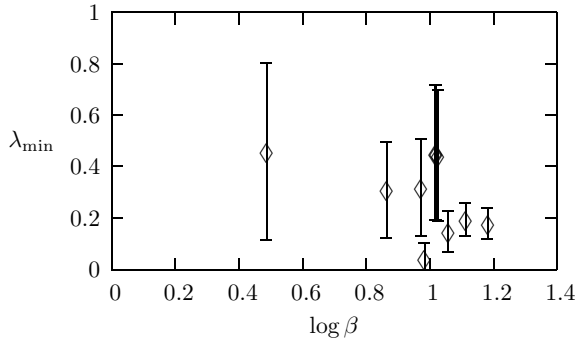

Figure 11. Projected angular rotation as a fraction of breakup velocity, λ, as a function of relative inverse radius β for extreme helium stars.

breakup as these stars contract towards the WD phase is much reduced compared with Fig. 9.

10 CONCLUSION

Assuming that angular momentum is strictly conserved within the system, we have calculated the rotation velocities of stars produced by the merger of WD binaries over a range of interesting initial mass ratios and possible outcomes. These include evolution through the giant phase, and subsequently towards either the WD or the helium main sequence. We have demonstrated that while it may be possible to produce the initial giants, the star (or its core) will spin-up as material is processed into the core or as the overall star contracts towards either of the compact configurations. This spin-up would be high enough to cause breakup.

More critically, the rotation velocities predicted under total conservation of angular momentum for post-giant objects are greater than those observed in the putative CO+He merger products, the extreme helium stars, by a factor of $\gtrsim$3.

Therefore, for the merger model to work, the star *must* lose angular momentum at some point in its evolution. The most likely time for this to occur is following formation of the disc after breakup of the secondary. In order to assume total conservation of angular momentum, it was necessary to assume that this disc is collisionless, but that assumption would also prevent the accretion of material on to the primary.

In fact, the completely opposite assumption must be considered. Lynden-Bell & Pringle (1974) argued that, in a viscous disc, angular momentum will be transported outwards while mass is transported inwards, on the viscous time-scale $\tau_{\rm visc} \approx R^2/\nu$, where R is the disc radius and ν the viscosity. The latter is approximately $(1/3)c_{\rm s}H$, where $c_{\rm s}$ is the sound speed and the scaleheight $H \approx Rc_{\rm s}/v_{\rm c}$, $v_{\rm c}$ being the Keplerian velocity for a circular orbit at radius R having a period P_R. Rearranging, we obtain $\tau_{\rm visc} \sim 3R/v_{\rm c}(R/H)^2$. If we take the disc radius to be approximately four times the WD radius, $R \sim 4\,R_{\rm wd}$, and the disc scaleheight to be twice the WD radius, we obtain $v_{\rm c} \approx 6R/P_R$ and $\tau_{\rm visc} \sim 2P_R \sim 500$ s. Such a mechanism provides a very efficient sink for the angular momentum, but poses a problem for the mass, which will be dumped on to the surface of the WD at a rate far in excess of the Eddington rate ($\dot{M}_{\rm Edd}$). Although accretion rates significantly higher than $\dot{M}_{\rm Edd}$ may be accommodated in a non-spherical geometry, for example, by accretion at the equator balanced by radiation in the polar axis, the disparity here seems to be insurmountable. Mass must be stored somewhere in the system where it is not supported by hydrostatic forces.

A hybrid solution might derive from a mechanism suggested first by Lynden-Bell & Pringle (1974) and explored again by Popham & Narayan (1991). This considers how material from an accretion disc would spin-up the accretor (note, this is a true accretion disc, and not a disrupted secondary). When the accretor reaches critical velocity, it interacts with the disc, actually spinning-up the disc. If this were to happen, then we could get momentum back into the disc, propagate it outwards and eject it from the outer edge of the disc.

A more detailed study of the dynamics of the binary disruption, disc formation and subsequent accretion is therefore warranted. Some progress has been made with smoothed particle hydrodynamics (Benz et al. 1990; Segretain et al. 1997; Geurrero et al. 2004); calculations have dealt principally with the dynamics of the secondary disintegration and subsequent disc formation, and give useful insight into the disc heating and mass distribution, that is, no explosion and negligible mass loss from the system. However, none goes far enough to establish the long-term outcome during and following disc accretion.

ACKNOWLEDGMENTS

KNG is grateful to the Armagh Observatory for a summer studentship during which this work was carried out. Research at the Armagh Observatory is funded by the Northern Ireland Department of Culture, Arts and Leisure. The authors are grateful to Prof. D. Lynden-Bell and Prof. M. E. Bailey for stimulating discussions.

REFERENCES

Benz W., Bowers R. L., Cameron A. G. W., Press W. H., 1990, ApJ, 348, 647
Chandrasekhar S., 1958, An Introduction to the Study of Stellar Structure. Dover Publications, New York
Chau W. Y., 1978, ApJ, 219, 1038
Eggleton P. P., 1983, ApJ, 268, 368
Geurrero J., García-Berro E., Isren J., 2004, A&A, 413, 257
Han Z., Webbink R. F., 1999, A&A, 349, L17
Iben I., Jr., 1990, ApJ, 353, 215
Iben I., Jr., Tutukov A. V., Yungelson L. R., 1996, ApJ, 456, 750
James R. A., 1964, ApJ, 140, 552
Jeffery C. S., 1993, A&A, 279, 188
Jeffery C. S., Heber U., 1993, A&A, 270, 167
Jeffery C. S., Hamill P. J., Harrison P. M., Jeffers S. V., 1998, A&A, 340, 476
Landau L., Lifshitz E., 1958, The Classical Theory of Fields. Pergamon, Oxford
Lynden-Bell D., Pringle J. E., 1974, MNRAS, 168, 603
Marsh T. R., 1995, MNRAS, 275, 1
Mohan C., Bayaty A. R., 1980, Ap&SS, 73, 227
Napiwotzki R., Karl C. A., Nelemans G. et al., 2005, in Koester D., Moehler S., eds, ASP Conf. Ser., Vol. 334, 14th European Workshop on White Dwarfs. Astron. Soc. Pac., San Francisco, p. 375
Nelemans G., Yungelson L. R., Portegies Zwart S. F., Verbunt F., 2001, A&A, 365, 491
Paczynski B., 1971, Acta Astron., 21, 1
Paczynski B., 1990, ApJ, 365, 9
Pandey G., Lambert D. L., Jeffery C. S., Rao N. K., 2006, ApJ, 638, 454
Panei J. A., Althaus L. G., Benvenuto O. G., 2000, A&A, 353, 970
Popham R., Narayan R., 1991, ApJ, 370, 604
Pringle J. E., 1981, ARA&A, 19, 137
Saio H., Jeffery C. S., 1988, ApJ, 328, 714
Saio H., Jeffery C. S., 2000, MNRAS, 313, 671
Saio H., Jeffery C. S., 2002, MNRAS, 333, 121
Segretain L., Chabrier G., Mochkovitch R., 1997, ApJ, 481, 355
Tassoul J. L., 1978, Theory of Rotating Stars. Princeton Univ. Press, Princeton, NJ
Vennes S., Fontaine G., Brassard P., 1995, A&A, 296, 117
Webbink R. F., 1984, ApJ, 277, 355

This paper has been typeset from a TEX/LATEX file prepared by the author.